LIMNOLOGY AND OCEANOGRAPHY
Letters

ASLO
Open Access

Limnology and Oceanography Letters 7, 2022, 167–174

doi: 10.1002/lol2.10222

LETTER

Always ready? Primary production of Arctic phytoplankton at the end of the polar night

Clara J. M. Hoppe *

Alfred-Wegener-Institut – Helmholzzentrum für Polar- und Meeresforschung, Bremerhaven, Germany

Scientific Significance Statement

The polar night with up to 6 months of darkness is a key characteristic of the Arctic Ocean, imposing unique challenges on phototrophic organisms like phytoplankton. These key primary producers have evolved different overwintering strategies to survive this extended dark period in winter. In situ data on their physiological state at the end of the polar night, and the effect of overwintering strategies on the spring bloom, are sparse. This study presents unprecedented physiological rate measurements from the Arctic transition phase between darkness and the return of the sun. It provides evidence that dominant polar phytoplankton keep their photosynthetic apparatus functionable over winter, and have a high capacity to efficiently use the returning sunlight, enabling high rates of chlorophyll *a* accumulation already in mid-February.

Abstract

The end of the polar night with the concurrent onset of photosynthetic biomass production ultimately leads to the spring bloom, which represents the most important event of primary production for the Arctic marine ecosystem. This dataset shows, for the first time, significant in situ biomass accumulation during the dark–light transition in the high Arctic, as well as the earliest recorded positive net primary production rates together with constant chlorophyll *a*-normalized potential for primary production through winter and spring. The results indicate a high physiological capacity to perform photosynthesis upon re-illumination, which is in the same range as that observed during the spring bloom. Put in context with other data, the results of this study indicate that also active cells originating from the low winter standing stock in the water column, rather than solely resting stages from the sediment, can seed early spring bloom assemblages.

In the polar oceans, several months of darkness prevent phototrophic biomass accumulation during winter. While traditionally, phototrophic organisms have been assumed to overwinter mainly in the form of resting stages, the presence of active cells in the water column in the middle of the polar night as well as the importance of mixotrophic lifestyle during low-light periods have been increasingly acknowledged in the recent years (Johnsen et al. 2020). Yet, knowledge on the

*Correspondence: clara.hoppe@awi.de

Associate editor: Marina Montresor

Author Contribution Statement: CJMH developed the research question and designed the study approach, conducted the field survey as well as the sample and data analysis, and wrote the paper.

Data Availability Statement: The presented data are available in the Pangaea data repository (Hoppe, CJM (2021): February phytoplankton ecophysiology in Kongsfjorden (79°N). https://doi.org/10.1594/PANGAEA.932880; Hoppe, CJM (2021): Photosynthetically active radiation during in situ incubations in February 2018 in Kongsfjorden (79°N). https://doi.org/10.1594/PANGAEA.932882.

ecophysiological characteristics of these assemblages is still rare. Measurements and experiments during the polar night in Svalbard indicate that phytoplankton are capable to reinitiate photosynthesis almost immediately upon re-illumination in the laboratory, even if in situ primary production is not measurable (Berge et al. 2015; Kvernvik et al. 2018). From experiments with single strains of polar phytoplankton, there is increasing evidence that species differ in the extent to which they manage to decrease metabolic energy needs in the dark as well as in their capacity to reestablish photosynthesis and growth upon re-illumination, yet overall capacities for recovery are remarkable (Kennedy et al. 2019; Lacour et al. 2019; Morin et al. 2019; van de Poll et al. 2020*a*). In view of this, it seems to be the return of sufficient sunlight (Cohen et al. 2020) for net growth rather than germination cues or molecular clocks that determines the start of phototrophic production.

The theoretical lower light limit of photosynthesis is with 0.01 μm photons m^{-2} s^{-1} quite low (Raven et al. 2000), but net pelagic phytoplankton growth has mostly been assumed to start at 1–5 μmol photons m^{-2} s^{-1} (Siegel et al. 2002; Boss and Behrenfeld 2010). More recently, extremely efficient usage of low light by Arctic phytoplankton and ice-algae with positive growth rates in extremely low-light environments of 0.17–0.25 μmol photons m^{-2} s^{-1} in and under sea ice have been observed (Hancke et al. 2018; Randelhoff et al. 2020). This is consistent with satellite-based observations that indicate that rates of biomass accumulation are actually highest in the early phase of Arctic spring, when biomass is still very low (Behrenfeld et al. 2017).

Due to logistic challenges, however, almost no discrete measurements of phytoplankton biomass development and productivity during the Arctic winter–spring transition exist (but *see* van de Poll et al. 2020b). To this end, surface chlorophyll *a* (Chl *a*) and particulate organic carbon (POC) concentrations as proxies for biomass as well as net primary production were measured at a coastal Arctic site (79°N, Svalbard, Norway) during the transition from polar night to daylight in February 2018.

Methods

Seawater sampling was conducted in February 2018 in Kongsfjorden, an open fjord on the west-coast of the Svalbard (Hop & Wiencke 2019). Due to logistical constrains so early in the year, sampling was conducted nearshore at 10 m water depth from the outer jetty of the harbor of Ny-Ålesund (78°55.72′N, 11°56.22′E) during a phase where no boat traffic occurred.

Average wind speed and incoming incident photosynthetically active radiation (PAR) were measured close to the nearby AWIPEV Atmospheric Observatory (Maturilli 2020). In short, a ThiesClima combined wind sensor was used to derive classic hourly averaged wind speed (m s^{-1}) were recorded at 10 m height. Hourly averaged incoming PAR in the range of 370–695 nm was calculated by subtracting UV and IR from the global incoming radiation, which was measured using pyranometers with different shading domes (Maturilli et al. 2019). Data were converted from planar measurements in (W m^{-2}) to scalar data in (μmol photons m^{-2} s^{-1}).

Manual conductivity-temperature-depth (CTD) profiles were collected with a *XR-620* CTD (RBR Ltd), equipped with a fluorescence sensor. Discrete samples from 0.5 m water depth were collected by single 5 L Niskin hauls. Samples for determination of total Chl *a* were gently vacuum-filtered (max. −200 kPa relative to atmosphere) onto precombusted (15 h, 500°C) GF/F filters (Whatman) and immediately frozen and stored at −20°C. For extraction, samples were placed in 6 mL 90% cooled acetone, homogenized using a cell mill (Precellys) and left overnight at −20°C. Chl *a* concentrations were determined on a fluorometer (Trilogy, Turner Designs), using an acidification step (1 M HCl) to determine phaeopigments Knap et al. (1996). Similar to Chl *a*, samples for POC and particulate organic nitrogen (PON) were gently vacuum-filtered onto precombusted GF/F filters and stored at −20°C. Samples were acidified with HCl to remove inorganic carbon and dried for at least 12 h at 60°C prior to sample preparation. Analysis was performed using a CHNS-O elemental analyzer (Euro EA 3000, HEKAtech).

Species presence was determined from samples collected with a small Apstein hand-net with 20 μm mesh size. The concentrated sample was transferred into a 50 mL falcon tube, fixed with Lugols solution (1% final concentration) and stored in the dark at 4°C. At the home laboratory, samples were settled for at least 24 h in an Uthermoehl chamber, and analyzed on an inverted light microscope (Axiovert Observer, Zeiss).

Potential net primary production rates were determined in duplicate 500 mL samples by incubation with $NaH^{14}CO_3$ spike (53.1 mCi $mmol^{-1}$; Perkin Elmer; applied specific activity of 0.5 μCi mL^{-1}) in unscratched 500 mL polycarbonate bottles (Nalgene) for 24 h under reference conditions (1.0 ± 0.6°C and 10 ± 3 μmol photons m^{-2} s^{-1}) together with a dark control. For in situ net primary production (NPP) (specific activity of 0.5 μCi mL^{-1}), two 500 mL samples were incubated at 0.2 m water depth in the harbor of Ny-Ålesund. Alongside with the polycarbonate incubation bottles, a miniPAR logger (PME) with a cosine-corrected underwater quantum sensor (LI-192, LICOR) was mounted to log the irradiances during the incubations. Please note that polycarbonate blocks UV, so that UV stress and inhibition were excluded. For both types of incubations, two 100 μL aliquots were mixed with 100 μL ethanolamine immediately after spiking to determine the total amount of added $NaH^{14}CO_3$. After 24 h, incubated samples were filtered onto GF/F filters, acidified with 200 μL of 1 M HCl and left to degas overnight. After addition of 10 mL of scintillation cocktail (Ultima Gold AB, PerkinElmer), samples were vortexed and left to stand in the dark for approximately 12 h before counting on the liquid

scintillation counter, using automatic quench correction and a counting time of 5 min. For blank determination, one replicate was immediately acidified with 0.5 mL 6 M HCl and treated as samples. Subtracted blank values were 25% ± 25% ($n = 23$) of the incubated sample counts. The disintegrations per minute of the dark control were subtracted from those of the light-incubated bottles. Potential and in situ NPP was calculated following Nielsen (1955).

Results and discussion

Surface phytoplankton Chl *a* concentrations and primary productivity were measured in February 2018 spanning the period when the sun reappears and raises over horizon on the 17th of February, that is, covering the official end of the polar night on Svalbard. Day length increased from less than 2 h on the 18th to more than 5 h on the 24th of February. During the sampling period, daily average incoming irradiance levels increased from 2 μmol photons m^{-2} s^{-1} on the 15th to 10 μmol photons m^{-2} s^{-1} on the 21st, with the irradiances between 22nd and 24th of February being lower due to cloud cover (5–7 μmol photons m^{-2} s^{-1}, Fig. 1A). At the same time, peak irradiances increased from 16 to 60 μmol photons m^{-2} s^{-1}.

During the first sampling on 15 February, surface Chl *a* concentrations were with 0.05 ± 0.001 μg L^{-1} (Fig. 1C) well above previously reported winter values 0.01–0.02 μg L^{-1} from Kongsfjorden (Berge et al. 2015; Hegseth et al. 2019), but below prebloom concentrations of 0.1–0.2 μg L^{-1} measured in the first half of April (Hegseth et al. 2019; van de Poll et al. 2020*b*; Hoppe et al. 2021). Manual CTD casts indicated no detectable stratification down to 9 m water depth (data not shown), but low daily average wind speeds of 2–5 m s^{-1} during the first week of the study (Fig. 1B) suggest the potential of a stabilization of the upper water column. In the following days, surface Chl *a* concentrations increased more than threefold to 0.18 ± 0.012 μg L^{-1} on 21 February. Exponential fitting indicated a Chl *a*-based specific growth rate constant of 0.46 d^{-1} ($R^2 = 0.98$), corresponding to a doubling of Chl *a* roughly every 36 h. As measured POC:Chl *a* ratios showed no clear trend (Table 1) Chl *a* may be used as a proxy for phytoplankton biomass for the short time span of this study. Such high POC:Chl *a* ratios, indicative a high nonphototrophic component of the particulate organic carbon pool, are commonly observed in high Arctic environments outside of bloom situations (Riedel et al. 2008; Campbell et al. 2016; Leu et al. 2020; Matthes et al. 2021). In combination with the observed increase in volume-based NPP, in situ as well as under reference conditions (Fig. 2), the development in Chl *a* (Fig. 1C) thus indicates significant biomass buildup during the polar night–day transition period.

While concurrent Chl *a* or biomass standing stocks cannot be estimated due to the lack of deeper samples further inside the fjord, the available data indicate nonetheless that phytoplankton can grow fast during this period (Fig. 1C). The resulting growth rate constant of 0.46 d^{-1} in the surface argues for an astonishingly high rate of biomass accumulation under such low light levels, exemplifying how efficiently Arctic phytoplankton can use light and exceed light compensation already at very low intensities. This is consistent with Randelhoff et al. (2020) who showed based on Argo float data that phytoplankton biomass accumulation in Baffin Bay (69–75°N) started already in February, so only days to weeks after the end of the polar night at this range of latitudes, despite snow and ice cover strongly reducing light availability in the surface ocean. Despite the similarity with regard to the early onset of biomass accumulation, the Chl *a*-derived growth rates in the latter study were more than an order of magnitude lower than those observed here, which likely stem from stronger light attenuation due to ice and snow cover in the study site of Randelhoff et al. (2020). Together, both studies emphasize that Arctic phytoplankton possess the abilities to perform photosynthesis under very low irradiances. The extent to which this actually occurs will depend on the specific environmental setting and the present phytoplankton assemblage.

After the period of low winds and increasing Chl *a* concentrations, daily wind speeds increased to values between 9 and 15 m s^{-1} during the 22nd to 24th of February (Fig. 1B). The peak of hourly wind speeds of 18 m s^{-1} (i.e., gale force) was measured in the night between 22nd and 23rd. After the storm, surface Chl *a* concentrations had decreased to values of 0.08 ± 0.002 μg L^{-1} on February 24th (Fig. 1C). This indicates that biomass accumulation was constrained to the surface waters before, and wind-induced mixing diluted the biomass. One should note that while water depth was shallow at the sampling location, the fjord is already deeper than 300 m less than 2 km from the shore (Tverberg et al. 2019). Given that Chl *a* concentrations after this strong wind event were still more than four times higher than those measured in the middle of the polar night, significant accumulation must have taken place even prior to the sampling, potentially from the beginning of the Civil Twilight (solar elevation above −6°; Cohen et al. 2020) on the first of February or even before. Given that wind speeds were low (Fig. 1) and wind directions came from rather southwesterly to southerly directions (Maturilli 2018), significant advection from the outside of the fjord seems rather unlikely (Cottier et al. 2007; Tverberg et al. 2019). Also, even if the biomass was laterally advected, it would still have been formed under very similar conditions as observed in this study, despite potentially even lower irradiances if originating from more deeply mixed waters outside the sheltered fjord.

To investigate primary production in surface waters during the study period, two incubations were conducted in situ at 0.2 m water depth. In the first incubation, that took place on the 15th of February under in situ daily average irradiances of 1.4 μmol photons m^{-2} s^{-1} and peak irradiances at 7.6 μmol

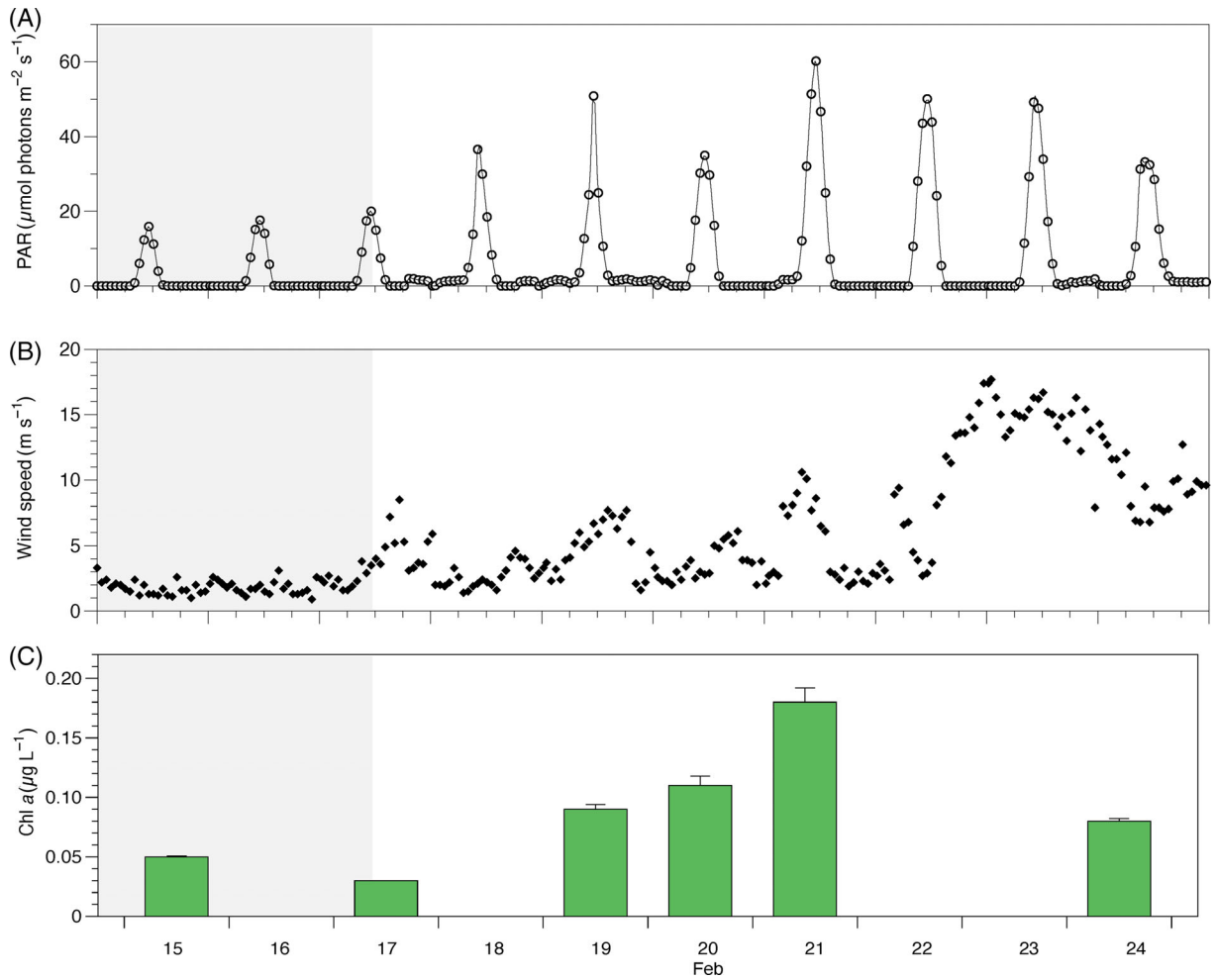

Fig. 1. Hourly incoming PAR (μmol photons m^{-2} s^{-1}) (**A**), and wind speeds (m s^{-1}) (**B**), as well as surface ocean Chl *a* concentrations (μg L^{-1}) in nearshore Kongsfjorden (**C**; $n = 2$ with one standard deviation except for February 17th, where $n = 1$) in February 2018. Gray shaded areas indicates polar night (solar elevation below −6°).

Table 1. Measured concentrations of particulate organic carbon (POC), POC:PON and POC:Chl *a* ratios as well as ^{14}C-based volumetric C-fixation data in the dark, in situ and under reference conditions (Ref) used for NPP estimates in surface waters of Kongsfjorden (79°N) in February.

Parameter	Unit	15 Feb 2018		19 Feb 2018		21 Feb 2018		24 Feb 2018	
Chl *a*	(μg L^{-1})	0.05	±0.001	0.09	±0.004	0.18	±0.011	0.08	±0.002
POC	(μg L^{-1})	63.88	na	na	na	63.27	na	60.21	na
POC:PON	(mol mol^{-1})	8.73	na	na	na	8.52	na	7.15	na
POC:Chl *a*	(g g^{-1})	1277	na	na	na	577	na	764	na
Dark C-fixation	(μmol C L^{-1} d^{-1})	0.001	na	0.003	na	0.004	na	na	na
In situ C-fixation	(μmol C L^{-1} d^{-1})	0.002	±0.001	na	na	0.013	±0.001	na	na
Ref C-fixation	(μmol C L^{-1} d^{-1})	0.005	±0.001	0.009	±0.002	0.020	±0.001	na	na

photons m^{-2} s^{-1} (Fig. 2E), in situ NPP was not detectable (Fig. 2B,D). Given the above-described Chl *a* increase from the 17th to the 19th as well as the as the fact that the machinery for light harvest and carbon fixation was present and activated (see below), the apparent lack in situ NPP is likely due to detection limits and uncertainties of the applied method

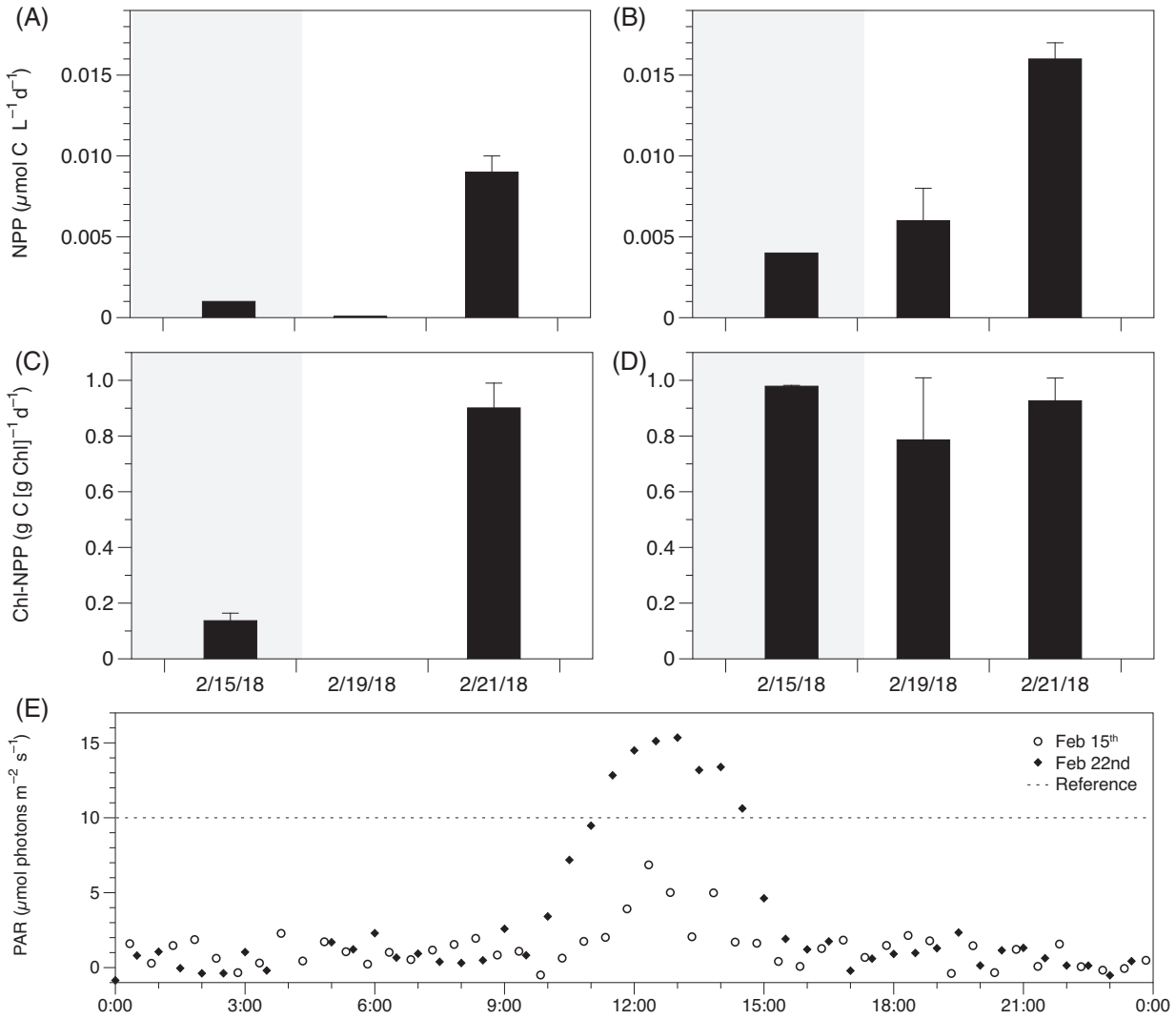

Fig. 2. ^{14}C-based volumetric NPP measured under in situ conditions (**A**) and reference conditions (**B**), as well as Chl *a*-specific NPP under in situ (**C**) and reference conditions (**D**) after subtraction of blank and dark values from C-fixation data (Table 1), and PAR (μmol photons m^{-2} s^{-1}) in the different incubations (**E**). Gray shaded areas indicates polar night (i.e., solar elevation below $-6°$).

($\pm$ 0.003 μmol C L^{-1} d^{-1} for the current dataset) rather than being truly zero. More sensitive methods would have to be used to prove either of these options. Moreover, it should be noted that, according to the manufacturer, the incubation bottles have an 80–90% light transmission capacity may have blocked some of the incoming light. Six days later, that is, on the 21st, rates had increased above the measurement uncertainty, now being 0.009 ± 0.001 μmol C L^{-1} d^{-1} and 0.90 ± 0.09 μg C (μg Chl *a*)$^{-1}$ d^{-1} for volume- and Chl *a*-specific estimates, respectively (Fig. 2B,2D). By then, the polar night had ended and daily average in situ irradiances were 3.0 μmol photons m^{-2} s^{-1}, with peak irradiances of 16.7 μmol photons m^{-2} s^{-1} (Fig. 2E). Please note that carbon fixation data estimated from dark incubations (Table 1), run in parallel to all incubations, was subtracted from the carbon fixation measurements in the light to derive NPP (Fig. 2). Dark fixation was with 0.004 μmol C L^{-1} d^{-1} in the same range as NPP on 15th of February, but only half as much as NPP on the 21st. Also, irradiances in the incubation bottes may have been 10–20% lower than in situ (see above), potentially making the measured rates even more astonishing. To my knowledge, this is the earliest positive in situ NPP ever measured in the Arctic spring (i.e., only 4 d after the end of the polar night).

To provide a better understanding of the observed in situ data, NPP was also measured under reference conditions of 1°C and 10 μmol photons m^{-2} s^{-1} over the study period. Volume-based reference-NPP increased from 0.004 ± 0.001 μmol C L^{-1} d^{-1} on the 15th to 0.016 ± 0.001 μmol C L^{-1} d^{-1} on the 21st of February (Fig. 2A), mirroring the development in Chl *a*. Similar to the in situ measurements, C-fixation in the dark was in the

same range as reference-NPP at the first sampling time point (i.e., 77%), but did not increase over time so that at the last time point, it accounted only for an additional 19% of C-fixation measured in the light (Table 1). When normalized to Chl *a*, however, C-fixation values ranged between 0.786 and 0.979 μg C (μg Chl *a*)$^{-1}$ d^{-1} without a temporal trend (Fig. 2C). This indicates that no substantial changes in photoacclimation and photosynthetic efficiency occurred over the study period. In fact, these values are in the same range to those derived from the subsequent spring bloom assemblage observed in April and May (0.88 ± 0.26 μg C (μg Chl *a*)$^{-1}$ d^{-1} at 10 μmol photons m^{-2} s^{-1}; Hoppe et al. 2021). Such surprisingly high rates of Chl *a*-specific carbon fixation indicate that Arctic phytoplankton either sustain fully functional and rather efficient photosystems throughout the polar night, or that they recover really quickly. Applying the same dark-control and normalization, the here measured values are even slightly lower than Chl *a*-specific NPP measured by Kvernvik et al. (2018) in the same study area in January, that is, in the middle of the polar night. These findings indicate an extraordinary ability of phytoplankton to sustain similar photosynthetic efficiencies throughout the most extreme changes in their environment, being a change from completely darkness to 24 h sunshine in spring. This is in line with laboratory experiments with the Arctic diatom *Chaetoceros neogracilis*, where growth rate measured after 1 month of darkness were only slightly influenced by the irradiances applied upon re-illumination (Lacour et al. 2019). It also fits into the increasing perception that Arctic coastal primary producers possess high capacities to compensate for environmental variability keeping species composition, ecophysiological parameters, and productivity comparably stable (Pančić et al. 2015; Hoppe et al. 2018*a*,*b*; Wolf et al. 2021, 2019). Whether or not some metabolic functions other than photosynthetic capacities still shift to some sort of resting mode is yet to be investigated.

A major drawback for understanding the conditions under which phytoplankton growth is initiated is that we currently do not have satisfactory estimates of phytoplankton respiration under different conditions (Behrenfeld and Boss 2018), despite knowing that respiration declines with decreasing irradiance (Geider et al. 1986; Halsey et al. 2010). Even though it seems plausible to assume relatively low costs of cell maintenance, especially of the photosynthetic apparatus, due to the cold and dark conditions, cells likely need alternative energy sources to survive the extended darkness of the polar night. Only some of the observed species and functional groups seem to be capable of phagotrophy, with the important group of diatoms not being able to use this energy source (McKie-Krisberg and Sanders 2014; Stoecker and Lavrentyev 2018; Jimenez et al. 2021). Osmotrophy, that is, the uptake of organic compounds from the surrounding seawater, on the other hand, seems to be a mechanism that all protists can employ to some degree (Worden et al. 2015; Mitra et al. 2016). Especially in a coastal system such as Kongsfjorden, where riverine and glacial runoff supply organic material, this seems a likely effective energy source.

Ratios of POC:N and POC:Chl *a* were determined on three occasions (Table 1) and showed rather high and variable values of 8.13 ± 0.86 mol C (mol N)$^{-1}$ and 873 ± 363 g C (g Chl *a*)$^{-1}$, respectively, indicating a substantial contribution of nonphototrophic particulate organic matter that is supported by mixo- and heterotrophic trophic modes. In line with high POC:Chl *a* ratios, light microscopic analysis indicated a mixed protist community composition of picoplankton (probably including single-celled *Micromonas pusilla*), unidentified flagellates (probably including single-celled *Phaeocystis pouchetii*) and diatoms (belonging to the genera of *Pseudo-Nitzschia*, *Pleurosigma*, *Entomoneis*, *Nitzschia*, *Licmophora*, and *Thalassiosira*) occurring together with ciliates and larger dinoflagellates. Thus, already at the end of the polar night, the same assemblages that usually also dominate the early spring bloom biomass in the study system were present (Hegseth et al. 2019); C. Hoppe unpubl. results). Furthermore, there is a significant overlap in the pelagic species composition with samples from December and January as well as in mid-March (Vader et al. 2015; Kvernvik et al. 2018). In April and May 2018, the Kongsfjorden spring bloom was in fact dominated by species that also occurred in winter, that is, diatoms such as *Nitzschia* and *Thalassiosira*, together with *Fragilariopsis* and *Navicula* during the exponential phase and flagellates such as *P. pouchetii* during the post-bloom phase (C. Hoppe unpubl. results). Thus, the present dataset indicates that, rather than having to be seeded from resting spores that overwinter in the surface sediment (Hegseth and Tverberg 2013), the spring bloom can also originate from this early assemblage that overwinters as active cells in the water column. This finding can fundamentally change the way we look at Arctic coastal overwintering and seeding mechanisms, and calls for a better understanding of their relative importance under different conditions. It also has implication for future projections, as active cells require more energy reserves than resting stages (McQuoid and Hobson 1996). Thus, winter energy demands of the former will increase more strongly with global warming and the increasing inflow of warmer Atlantic waters into the Arctic, putting this overwintering strategy at risk.

In conclusion, this dataset provides unprecedented insight into the overwintering strategies of Arctic phytoplankton and the initiation of its spring blooms. It also urges us to develop a better understanding of the physiological adaptations to prolonged darkness, for example, with respect to alternative energy sources of active cells, germination cues of resting stages and reinitiation mechanisms of photosynthesis. The ability to acclimate to and thrive in such low light environments, as studied here, indicates a large potential of primary production to occur also in the extensive twilight areas of the world's oceans. This new knowledge will also be very valuable for improving parameterizations of primary productivity in

biogeochemical and ecological models. The surprisingly early and high rates of biomass production together with the persistence of the phytoplankton assemblage in terms of photosynthetic efficiency and species composition throughout winter and spring showcases the high capacities of Arctic phytoplankton to compensate for large ranges of environmental variability. In the high North, there seem to always be phytoplankton that is ready to capture and efficiently use the scarce and only periodically available key resource of light and thus most likely did not specifically adapt to the polar night.

References

Behrenfeld, M. J., and E. S. Boss. 2018. Student's tutorial on bloom hypotheses in the context of phytoplankton annual cycles. Glob. Change Biol. **24**: 55–77. doi:10.1111/gcb.13858

Behrenfeld, M. J., and others. 2017. Annual boom–bust cycles of polar phytoplankton biomass revealed by space-based lidar. Nat. Geosci. **10**: 118–122. doi:10.1038/ngeo2861

Berge, J., and others. 2015. Unexpected levels of biological activity during the polar night offer new perspectives on a warming Arctic. Curr. Biol. **25**: 2555–2561. doi:10.1016/j.cub.2015.08.024

Boss, E., and M. Behrenfeld. 2010. In situ evaluation of the initiation of the North Atlantic phytoplankton bloom. Geophys. Res. Lett. **37**: L18603. doi:10.1029/2010GL044174

Campbell, K., C. J. Mundy, J. C. Landy, A. Delaforge, C. Michel, and S. Rysgaard. 2016. Community dynamics of bottom-ice algae in Dease Strait of the Canadian Arctic. Prog. Oceanogr. **149**: 27–39. doi:10.1016/j.pocean.2016.10.005

Cohen, J. H., J. Berge, M. A. Moline, G. Johnsen, and A. P. Zolich. 2020. Light in the polar night, p. 37–66. *In* J. Berge, G. Johnsen, and J. H. Cohen [eds.], *POLAR NIGHT marine ecology: Life and light in the dead of night*. Springer International Publishing. doi:10.1007/978-3-030-33208-2_3

Cottier, F. R., F. Nilsen, M. E. Inall, S. Gerland, V. Tverberg, and H. Svendsen. 2007. Wintertime warming of an Arctic shelf in response to large-scale atmospheric circulation. Geophys. Res. Lett. **34**: L10607. doi:10.1029/2007GL029948

Geider, R. J., B. A. Osbonie, and J. A. Raven. 1986. Growth, photosynthesis and maintenance metabolic cost in the diatom *Phaeodactylum tricornutum* at very low light levels. J. Phycol. **22**: 39–48. doi:10.1111/j.1529-8817.1986.tb02513.x

Halsey, K., A. Milligan, and M. Behrenfeld. 2010. Physiological optimization underlies growth rate-independent chlorophyll-specific gross and net primary production. Photosynth. Res. **103**: 125–137. doi:10.1007/s11120-009-9526-z

Hancke, K., L. C. Lund-Hansen, M. L. Lamare, S. Højlund Pedersen, M. D. King, P. Andersen, and B. K. Sorrell. 2018. Extreme low light requirement for algae growth underneath sea ice: A case study from Station Nord, NE Greenland. J. Geophys. Res. Oceans **123**: 985–1000. doi:10.1002/2017JC013263

Hegseth, E. N., and V. Tverberg. 2013. Effect of Atlantic water inflow on timing of the phytoplankton spring bloom in a high Arctic fjord (Kongsfjorden, Svalbard). J. Mar. Syst. **113–114**: 94–105. doi:10.1016/j.jmarsys.2013.01.003

Hegseth, E. N., and others. 2019. Phytoplankton seasonal dynamics in Kongsfjorden, Svalbard and the adjacent shelf, p. 173–227. *In* H. Hop and C. Wiencke [eds.], *The ecosystem of Kongsfjorden, Svalbard*. Springer. doi:10.1007/978-3-319-46425-1_6

Hop, H., and Wiencke, C., 2019. The Ecosystem of Kongsfjorden, Svalbard. In *Advances in Polar Ecology*. Springer. doi:10.1007/978-3-319-46425-1.

Hoppe, C. J. M., L. Wischnewski, K. K. E. Wolf, C. Finlo, and B. Rost. 2021. Biogeochemical and ecophysiological monitoring at station KB3 in Kongsfjorden (2014–2018). doi:10.1594/PANGAEA.931854

Hoppe, C. J. M., K. K. E. Wolf, N. Schuback, P. D. Tortell, and B. Rost. 2018*b*. Compensation of ocean acidification effects in Arctic phytoplankton assemblages. Nat. Clim. Change **8**: 529–533. doi:10.1038/s41558-018-0142-9

Hoppe, C. J. M., and others. 2018*a*. Resistance of Arctic phytoplankton to ocean acidification and enhanced irradiance. Polar Biol. **41**: 399–413. doi:10.1007/s00300-017-2186-0

Jimenez, V., J. A. Burns, F. Le Gall, F. Not, and D. Vaulot. 2021. No evidence of Phago-mixotropy in *Micromonas polaris* (Mamiellophyceae), the dominant Picophytoplankton species in the Arctic. J. Phycol. **57**: 435–446. doi:10.1111/jpy.13125

Johnsen, G., E. Leu, and R. Gradinger. 2020. Marine micro- and macroalgae in the polar night, p. 67–112. *In* J. Berge, G. Johnsen, and J. H. Cohen [eds.], *POLAR NIGHT marine ecology: Life and light in the dead of night*. Springer International Publishing. doi:10.1007/978-3-030-33208-2_4

Kennedy, F., A. Martin, J. P. Bowman, R. Wilson, and A. McMinn. 2019. Dark metabolism: A molecular insight into how the Antarctic sea-ice diatom *Fragilariopsis cylindrus* survives long-term darkness. New Phytol. **223**: 675–691. doi:10.1111/nph.15843

Knap, A., A. Michaels, A. Close, H. Ducklow, and A. Dickson [eds.]. 1996. Protocols for the Joint Global Ocean Flux Study (JGOFS) core measurements, JGOFS Report Nr. 19. UNESCO.

Kvernvik, A. C., C. J. M. Hoppe, E. Lawrenz, O. Prášil, M. Greenacre, J. M. Wiktor, and E. Leu. 2018. Fast reactivation of photosynthesis in arctic phytoplankton during the polar night. J. Phycol. **54**: 461–470. doi:10.1111/jpy.12750

Lacour, T., P.-I. Morin, T. Sciandra, N. Donaher, D. A. Campbell, J. Ferland, and M. Babin. 2019. Decoupling light harvesting, electron transport and carbon fixation during prolonged darkness supports rapid recovery upon re-illumination in the Arctic diatom Chaetoceros neogracilis. Polar Biol. **42**: 1787–1799. doi:10.1007/s00300-019-02507-2

Leu, E., and others. 2020. Spatial and temporal variability of ice algal trophic markers—with recommendations about their application. J. Mar. Sci. Eng. **8**: 676. doi:10.3390/jmse8090676

Matthes, L. C., and others. 2021. Environmental drivers of spring primary production in Hudson Bay. Elem. Sci. Anthr. **9**: 00160. doi:10.1525/elementa.2020.00160

Maturilli, M. 2018. Continuous meteorological observations at station Ny-Ålesund (2018-02). Alfred Wegener Institute - Research Unit Potsdam. doi:10.1594/PANGAEA.894665

Maturilli, M., Hanssen-Bauer, I., Neuber, R., Rex, M., and Edvardsen, K., 2019. The Atmosphere Above Ny-Ålesund: Climate and Global Warming, Ozone and Surface UV Radiation, p. 23–46. In *The Ecosystem of Kongsfjorden, Svalbard*, Springer. doi:10.1007/978-3-319-46425-1_2.

Maturilli, M. 2020. Basic and other measurements of radiation at station Ny-Ålesund (2006–05 et seq).

McKie-Krisberg, Z. M., and R. W. Sanders. 2014. Phagotrophy by the picoeukaryotic green alga *Micromonas*: Implications for Arctic Oceans. ISME J. **8**: 1953–1961. doi:10.1038/ismej.2014.16

McQuoid, M. R., and L. A. Hobson. 1996. Diatom resting stages. J. Phycol. **32**: 889–902. doi:10.1111/j.0022-3646.1996.00889.x

Mitra, A., and others. 2016. Defining planktonic protist functional groups on mechanisms for energy and nutrient acquisition; incorporation of diverse mixotrophic strategies. Protist **167**: 106–120. doi:10.1016/j.protis.2016.01.003

Morin, P.-I., and others. 2019. Response of the sea-ice diatom *Fragilariopsis cylindrus* to simulated polar night darkness and return to light. Limnol. Oceanogr. **65**: 1041–1060. doi:10.1002/lno.11368

Nielsen, E. S. 1955. The interaction of photosynthesis and respiration and its importance for the determination of 14C-discrimination in photosynthesis. Physiol. Plant. **8**: 945–953. doi:10.1111/j.1399-3054.1955.tb07790.x

Pančić, M., P. J. Hansen, A. Tammilehto, and N. Lundholm. 2015. Resilience to temperature and pH changes in a future climate change scenario in six strains of the polar diatom *Fragilariopsis cylindrus*. Biogeosciences **12**: 4235–4244. doi:10.5194/bg-12-4235-2015

van de Poll, W. H., E. Abdullah, R. J. W. Visser, P. Fischer, and A. G. J. Buma. 2020*a*. Taxon-specific dark survival of diatoms and flagellates affects Arctic phytoplankton composition during the polar night and early spring. Limnol. Oceanogr. **65**: 903–914. doi:10.1002/lno.11355

van de Poll, W. H., D. S. Maat, P. Fischer, R. J. W. Visser, C. P. D. Brussaard, and A. G. J. Buma. 2020*b*. Solar radiation and solar radiation driven cycles in warming and freshwater discharge control seasonal and inter-annual phytoplankton chlorophyll a and taxonomic composition in a high Arctic fjord (Kongsfjorden, Spitsbergen). Limnol. Oceanogr. **66**: 1221–1236. doi:10.1002/lno.11677

Randelhoff, A., and others. 2020. Arctic mid-winter phytoplankton growth revealed by autonomous profilers. Sci. Adv. **6**: eabc2678. doi:10.1126/sciadv.abc2678

Raven, J. A., J. E. Kübler, and J. Beardall. 2000. Put out the light, and then put out the light. J. Mar. Biol. Assoc. U. K. **80**: 1–25. doi:10.1017/S0025315499001526

Riedel, A., C. Michel, M. Gosselin, and B. LeBlanc. 2008. Winter–spring dynamics in sea-ice carbon cycling in the coastal Arctic Ocean. J. Mar. Syst. **74**: 918–932. doi:10.1016/j.jmarsys.2008.01.003

Siegel, D. A., S. C. Doney, and J. A. Yoder. 2002. The North Atlantic spring phytoplankton bloom and Sverdrup's critical depth hypothesis. Science **296**: 730–733. doi:10.1126/science.1069174

Stoecker, D. K., and P. J. Lavrentyev. 2018. Mixotrophic plankton in the polar seas: A pan-Arctic review. Front. Mar. Sci. **5**: 292. doi:10.3389/fmars.2018.00292

Tverberg, V., and others. 2019. The Kongsfjorden transect: Seasonal and inter-annual variability in hydrography, p. 49–104. *In The ecosystem of Kongsfjorden, Svalbard*. Springer.

Vader, A., M. Marquardt, A. R. Meshram, and T. M. Gabrielsen. 2015. Key Arctic phototrophs are widespread in the polar night. Polar Biol. **38**: 13–21. doi:10.1007/s00300-014-1570-2

Wolf, K. K. E., E. Romanelli, B. Rost, U. John, S. Collins, H. Weigand, and C. J. M. Hoppe. 2019. Company matters: The presence of other genotypes alters traits and intraspecific selection in an Arctic diatom under climate change. Glob. Change Biol. **25**: 2869–2884. doi:10.1111/gcb.14675

Wolf, K. K. E., and others. 2021. Revealing environmentally driven population dynamics of an Arctic diatom using a novel Microsatellite PoolSeq Barcoding approach. Environ. Microbiol. **23**: 3809–3824. doi:10.1111/1462-2920.15424

Worden, A. Z., M. J. Follows, S. J. Giovannoni, S. Wilken, A. E. Zimmerman, and P. J. Keeling. 2015. Rethinking the marine carbon cycle: Factoring in the multifarious lifestyles of microbes. Science **347**: 1257594. doi:10.1126/science.1257594

Acknowledgments

This work would have not been possible without the field support by Rodolphe Merceron and the rest of the AWIPEV station team 2017/18. Marion Maturilli is acknowledged for the provision of PAR and wind data from the AWIPEV Atmospheric Observatory, and Marcel Machnik for assistance with POC/PON measurements. Special thanks to Björn Rost as well as the editors and reviewers for providing valuable feedback to an earlier version of this manuscript. The author declares no competing interests. I acknowledge support by the Open Access Publication Funds of Alfred-Wegener-Institut Helmholtz- Zentrum für Polar- und Meeresln-forschung. Open Access funding enabled and organized by Projekt DEAL.

Submitted 01 June 2021
Revised 29 September 2021
Accepted 15 October 2021